CATALYSIS

The oscillating Fischer-Tropsch reaction

Rui Zhang[1], Yong Wang[1,2]*, Pierre Gaspard,[3] Norbert Kruse[1,2,4]*

The mechanistic steps that underlie the formation of higher hydrocarbons in catalytic carbon monoxide (CO) hydrogenation at atmospheric pressure over cobalt-based catalysts (Fischer-Tropsch synthesis) have remained poorly understood. We reveal nonisothermal rate-and-selectivity oscillations that are self-sustained over extended periods of time (>24 hours) for a cobalt/cerium oxide catalyst with an atomic ratio of cobalt to cerium of 2:1 (Co_2Ce_1) at 220°C and equal partial pressures of the reactants. A microkinetic mechanism was used to generate rate-and-selectivity oscillations through forced temperature oscillations. Experimental and theoretical oscillations were in good agreement over an extended range of reactant pressure ratios. Additionally, phase portraits for hydrocarbon production were constructed that support the thermokinetic origin of our rate-and-selectivity oscillations.

The hydrogenation of carbon monoxide to chain-lengthened hydrocarbons was initially reported by BASF company in 1913, where the reaction occurred under hydrogen-deficient synthesis conditions (*1*). A decade later, Fischer and Tropsch (*2*) demonstrated hydrocarbon synthesis from stoichiometric mixtures with H_2/CO ratios of 2 (or even more H_2-rich mixtures) that were compatible with the "syngas" derived from coal gasification and adjusted by water gas shift. Mainly iron and cobalt metal particles on a suitable support material were found to be active catalysts. The underlying mechanistic steps of this polymerization-type surface reaction are still under debate more than 100 years later. No consensus has emerged on the chain-lengthening mechanism that leads to hydrocarbons and their functionalized derivatives, in part because of metal-support synergies that range from weak interactions to strong chemical bonding and compound formation. Also, structural and chemical reconstruction effects on both the surface and in the bulk of the catalytically active metals (*3*–*12*) further complicate mechanistic studies.

Recent experimental studies have demonstrated that an all-embracing reaction mechanism to produce paraffins, olefins, and oxygenates (mainly alcohols and aldehydes) is unlikely to exist. Besides metal-support interactions, process temperatures and variable syngas compositions at atmospheric and elevated pressure conditions affect the mechanistic pathways. In this context, we note that Fischer originally adopted the view of a "formate-type" intermediate (*2*) after the report by Christiansen (*13*) of the catalytic hydrogenation of methyl formate to methanol. However, Fischer soon discarded this possibility after realizing that excessive carbon deposition from CO over alkali-promoted iron catalysts would lead to the formation of metal carbides prone to undergoing hydrogenation to hydrocarbons. Much of the present-day research favors a "carbide-type" mechanism that involves C–C coupling of CH_x intermediates. However, experimental evidence has also been presented for a CO insertion mechanism under steady-state conditions of the Fischer-Tropsch (FT) process (*14*–*20*). This mechanism benefits from its ability to account for the formation of chain-lengthened oxygenates besides paraffins and olefins. Reducible oxides of metals, in particular, those containing manganese, have been demonstrated to

[1]Voiland School of Chemical Engineering and Bioengineering at Washington State University, Pullman, WA 99164, USA. [2]Institute for Integrated Catalysis, Pacific Northwest National Laboratory, Richland, WA 99332, USA. [3]Centre for Nonlinear Phenomena and Complex Systems, CP231, Université Libre de Bruxelles, B-1050 Brussels, Belgium. [4]Chemistry of Surfaces, Interfaces and Nanomaterials (ChemSIN), CP243, Université Libre de Bruxelles, B-1050 Brussels, Belgium.
*Corresponding author. Email: norbert.kruse@wsu.edu (N.K.); wang42@wsu.edu (Y.W.)

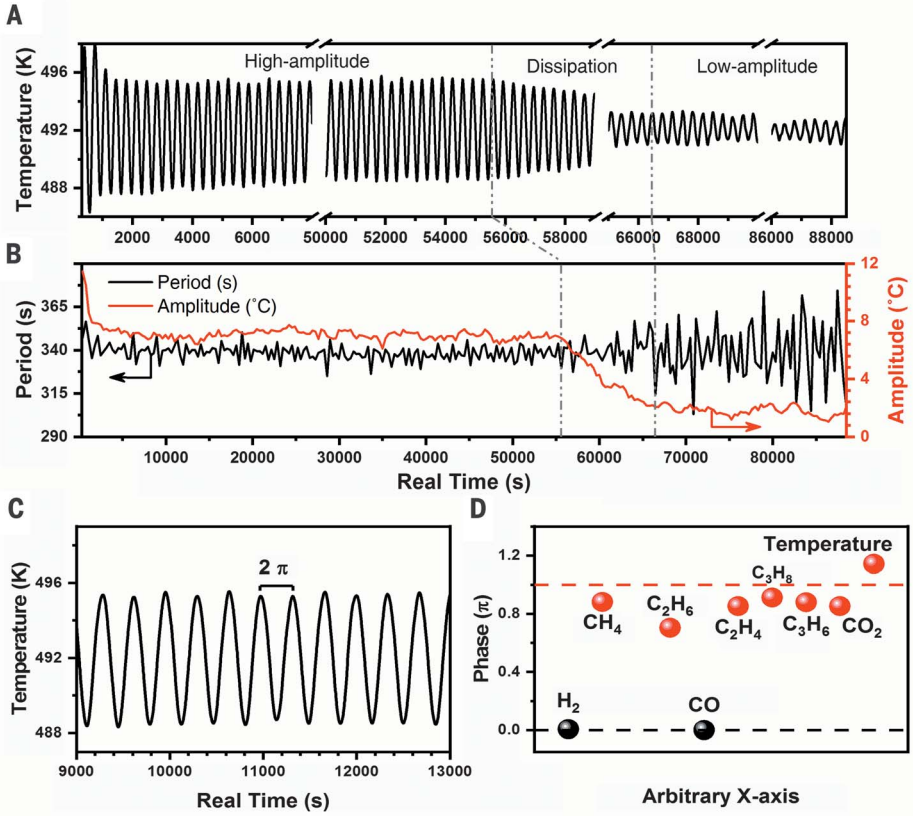

Fig. 1. Oscillatory behavior in the FT reaction. (**A** to **D**) Self-sustained long-term oscillations of the temperature over a Co/Ce–oxide catalyst of Co_2Ce_1 atomic composition at 220°C, 1 bar total pressure, and a H_2/CO ratio of 1/1. Oscillating temperatures (A) with periods of about 340 s and amplitudes of 7 Celsius degrees (for 16 hours) and 2 Celsius degrees (6 hours) (B) are observed along with a "dissipation" period in between and a short final dying-out. The harmonicity of the temperature oscillations is demonstrated in (C), and phases of temperature are related to those of the reactants and selected products after Fourier transformation in (D). Black and red dashed lines represent relative phases zero and π. C_4 products show the same behavior.

strongly promote the catalytic performance of cobalt-based catalysts (*9–12*, *21*, *23–25*). Rate-and-selectivity hysteresis driven by a Co-to-Co_2C reaction-induced structural transformation has been reported for the high-pressure synthesis of chain-lengthened paraffins, olefins, alcohols, and aldehydes (*25*). Recent reports on using CeO_2 in Co-based catalyst formulations (*26*) highlighted the occurrence of a strong metal-support interaction (*27–29*) that led to the formation of patchy capping overlayers with enriched metal/CeO_x interface structures that serve as potential reaction sites (*30*). These insights challenged the authoritative view of Iglesia *et al.* (*31*) that hydrocarbon synthesis over Co-based catalysts is support independent.

Although time-dependent reaction kinetics to the point of hysteresis and oscillations were already demonstrated in the early 1970s for the CO oxidation over Pt-based catalysts (*32*, *33*), little is known so far about such kinetic instabilities in reaction networks as complicated as the catalytic CO hydrogenation. Because of possible heat- and mass-transfer limitations in solid catalysts, oscillations are usually nonisothermal. Indeed, Tsotsis *et al.* (*34*) observed temperature variations of up to 200 Celsius degrees in the CO hydrogenation over Fe/zeolite catalysts of poor thermal conductivity. In this work, we report periodic rate-and-selectivity oscillations in the FT reaction over a Co/Ce–oxide powder catalyst. Temperature amplitudes of several Celsius degrees were observed and were correlated to the periodic activity-and-selectivity changes of the Co/Ce–oxide catalyst. The experimental evidence allowed us to develop a mechanistic framework that shows how observed oscillatory reactions can be generated through periodic temperature forcing. We also present phase portraits for oscillatory reactant and product formation in agreement with the thermokinetic origin of our observations.

Experimental studies

We used a fixed-bed flow reactor designed to minimize concentration gradients of reactants and products to allow the reactor response to be monitored as a function of time when switching reactant flows between different compositions. In the present study, such a transient response was obtained after swiftly replacing a H_2 flow (for catalyst activation and to provide a metallic Co phase) in He with a reactive syngas mixture of H_2/CO in argon. Noble gases were used as balance and reference along with an independent flow of Ne that bypassed the reactor to allow molecular flows of reactants and products to be calculated, assuming negligible concentration gradients in the reactor and laminar flow in the pipes leading to the analytical devices. The experimental procedure that we adopted to generate rate-and-selectivity oscillations of the atmospheric-pressure FT reaction over Co/ceria is shown in fig. S1.

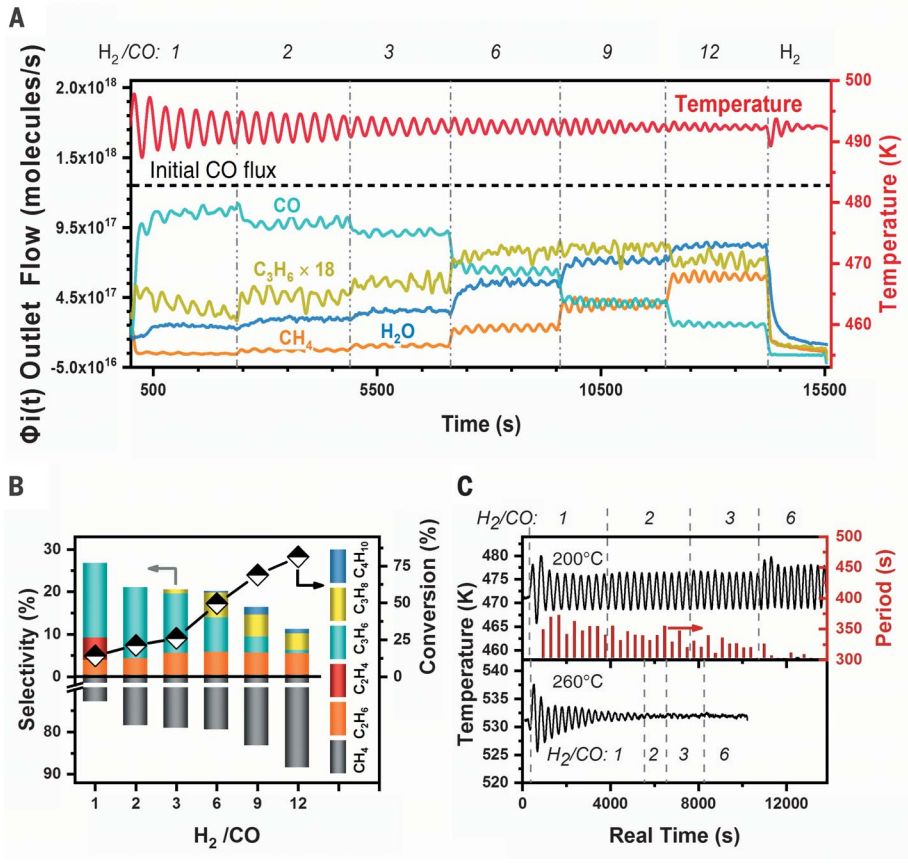

Fig. 2. Effect of H_2/CO ratio and temperature on the oscillatory behavior over a Co/Ce–oxide catalyst with Co_2Ce_1 atomic composition. (**A**) Evolution of temperature and rate-and-selectivity oscillations (as reactor outlet flows of reactants and products) as a function of the H_2/CO ratio at a nominal temperature of 220°C. The horizontal black dashed line represents the CO molecular flow into the reactor and serves to calculate time-averaged reaction rates. Dashed vertical lines distinguish reactant ratios between H_2/CO = 1 and 12. ϕi(t), reactor outlet flow. (**B**) CO conversion and product selectivities for varying H_2/CO ratios at 220°C. (**C**) Time evolution of oscillations at 200°C (top) and 260°C (bottom) for selected H_2/CO ratios. Red bars in the top graph reflect the variation of the oscillation period with time and the H_2/CO ratio.

After reducing conditions in H_2 switched to reactive conditions in H_2/CO, while the flow rate was kept constant, the catalytically active surface phase began to form. Such chemical conditioning always preceded the onset of oscillations and was associated with delay times of some hundreds of seconds, depending on the actual H_2/CO ratio (which varied from 1 to 12) and Co/Ce atomic ratios in Co/Ce–oxide catalysts (Co/Ce atomic ratios varied from 0.5 to 4). For the conditions shown in Fig. 1, long-term oscillations in temperature with periods of about 340 s and amplitudes of ~7 Celsius degrees were obtained for Co/Ce = 2 and H_2/CO = 1. After 15 hours, the amplitudes decreased to ~2 Celsius degrees (Fig. 1, A and B, and fig. S3). Such changes in amplitude were not abrupt but rather sluggish and occurred on timescales of ~1 hour. The origin of amplitude damping is not clear but could be associated with changes in the surface composition of the

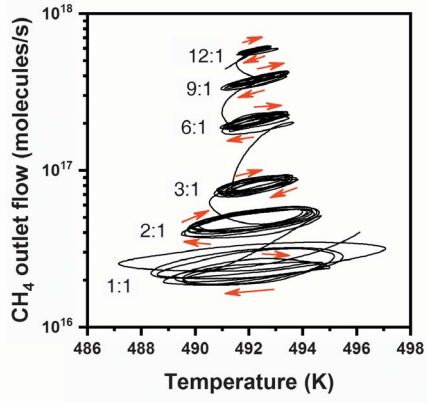

Fig. 3. Phase portrait of CH_4 selectivity versus temperature at different H_2/CO ratios. The experimental conditions are the same as in Fig. 2. Phase portraits, or phase-space trajectories, are constructed from extended time series of the oscillating product flows. Transitions to higher cycles are caused whenever the H_2/CO ratio is increased. The red arrows indicate the direction of time evolution.

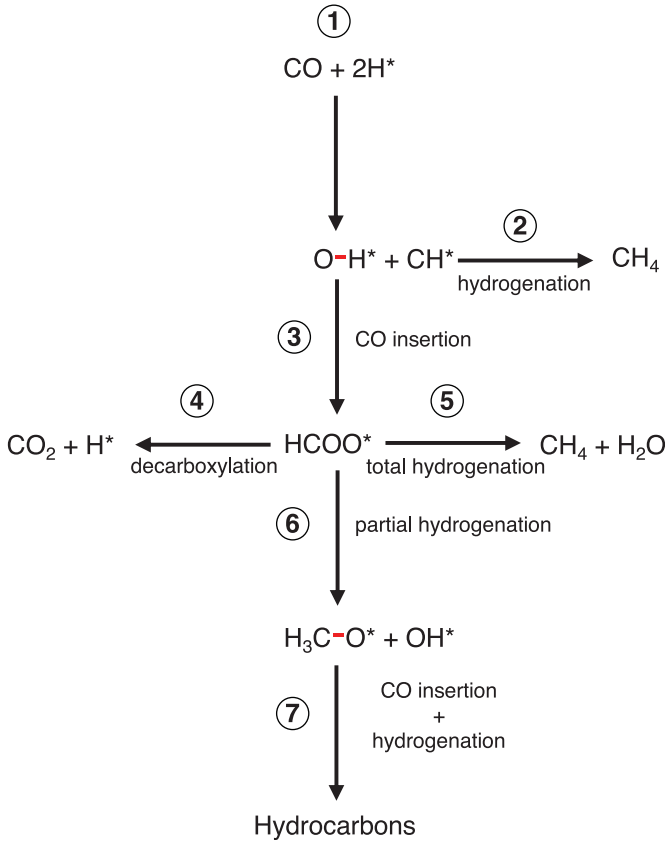

Fig. 4. Reduced reaction scheme that underlies theoretical modeling with forced temperature oscillations. Chain lengthening involves CO insertion into O–H or O–R bonds of surface hydroxy or alkoxy, respectively (critical bonds are highlighted in red). Methane formation occurs through either an "early" pathway via CH_x hydrogenation or a "late" pathway involving hydrogenation of surface formate. Only the late pathway develops oscillatory behavior, as do higher hydrocarbons. Generally, the reaction scheme lumps together several elementary steps to enable the mathematical treatment. Water gas shift is an integral part of the scheme. Possible surface reconstructions (due to Co-to-Co_2C or CeO_2-to-Ce_2O_3 chemical transformations) have not been considered, in accordance with x-ray diffraction results shown in fig. S7. The details of this reaction scheme along with the kinetic approach can be found in the supplementary materials.

catalyst from the adsorption of contaminating species.

Oscillating temperatures reflected periodic changes in the exothermicity of the reaction. In Fig. 1C, we show a selected time window to exemplify the harmonicity of the high-amplitude oscillations. Thermal coupling between remote catalyst particles had to be highly efficient to ensure the apparently concerted reaction behavior across the catalyst bed. In this context, no oscillatory behavior was observed after replacing Ar with He as the vector gas. The fast heat exchange between catalyst particles and gas phase that is enabled by the high thermal conductivity of He was lost after replacement with Ar (for details, see the supplementary materials).

Phase differences between temperature oscillations and reactants and products (Fig. 1D) showed that temperature maxima and minima correlated with enhanced and reduced product formation, respectively, whereas reactants were out of phase with both temperature and products. These interdependencies were also apparent from phase portraits, as will be shown for the case of methane formation.

Figure 2 demonstrates the oscillatory behavior as a function of the H_2/CO pressure ratio and temperature. Although this pressure ratio has been set to between 1 and 3 in most investigations of the FT reaction, we have chosen to extend it up to 12 after our previous studies over Co/Mn–oxide catalysts, which showed rate and selectivity hysteresis to endure a large excess of H_2 (*25*). Figure 2A demonstrates the exceedingly broad existence range of temperature and selected chem-species' oscillations as the H_2/CO ratio varies from 1 to 12. As this ratio is increased from low to high, the oscillation period decreased from ~340 to ~230 s and the amplitude decreased from 7 to 1 Celsius degree, respectively (fig. S3). Time-averaged reactor outlet flows decreased for CO and increased for all product species (exemplified for methane and propene in Fig. 2A), as expected for more-reducing reaction conditions.

Although the CO conversion increased from an initial value of 14% at H_2/CO = 1 to a final value of 81% at H_2/CO = 12, the product species exhibited a more-differentiated picture (Fig. 2B). Less-hydrogenated species, such as olefins, were formed preferentially at low H_2/CO ratios, as had been reported for promoted Co/Mn–oxide catalysts in the absence of long-term oscillations (*9*, *10*, *23*). According to high-resolution electron microscopy studies, a Co-to-Co_2C phase transformation occurred under these hydrogen-deficient conditions (*9*, *10*). Olefin formation, especially for ethylene, decreased at increasing H_2/CO ratios (Fig. 2B). The formation of methane, the most hydrogenated product, became dominant at higher H_2/CO ratios and reached ~90% selectivity at H_2/CO = 12. Although some chain lengthening to C_{2+} paraffins was retained, early chain termination was favored under these strongly reducing conditions.

Figure 2C illustrates that the oscillatory behavior described so far only occurred within a limited range of temperatures. At 200°C, regular oscillations were observed over a wide range of H_2/CO pressure ratios. Similar to observations made for a reaction temperature of 220°C (as mentioned earlier), oscillation periods decreased with increasing H_2/CO ratio. At 260°C, oscillations with fading amplitude were observed for H_2/CO = 1. The dissipation was then followed by the extinction of any oscillatory behavior at higher H_2/CO ratios. We note that Co/Ce–oxide catalysts with Co/Ce atomic compositions that were appreciably different from 2 (Co/Ce = 0.5, for example; see fig. S4) did not exhibit oscillatory behavior (fig. S4).

The phase-space trajectories of the methane outlet flow versus temperature are shown in Fig. 3. For each H_2/CO ratio, the trajectory formed a cycle with the orientation expected for a mechanism of thermokinetic instability (*35*, *36*). In this mechanism, a thermokinetic feedback caused by the high exothermicity of the FT reaction produced an increase of the temperature and an acceleration in the consumption of the adsorbed reactants, which then slowed the reaction and closed the cycle. In this way, the thermokinetic instability may trigger self-sustained oscillations (*37*), as observed in our research and described above.

Theoretical analysis

A deeper understanding of the intrinsically time-dependent reaction kinetics described thus far required a theoretical analysis of the reaction mechanism, the details of which are presented in the supplementary materials. A reduced scheme that summarizes the essential aspects of this mechanism is shown in Fig. 4. In particular, we assume hydrogen-assisted dissociation of CO (*15*, *38*) to provide O–H surface hydroxyl and partially hydrogenated carbon species, followed by hydrogenation of the latter to produce methane. Importantly, the O–H bond of OH undergoes an insertion reaction with CO to form surface formate-type species as a key surface reaction intermediate. A similar reaction scenario has also been envisaged for the methanol synthesis (*39*–*41*) over Cu-based catalysts. However, potential variations in the denticity of surface-bound formate, which could lead to different reactivities (*42*, *43*), have not been considered in our reaction scheme. The occurrence of CO insertion in the atmospheric FT reaction has been previously demonstrated in chemical transient studies using Co/MgO (*14*),

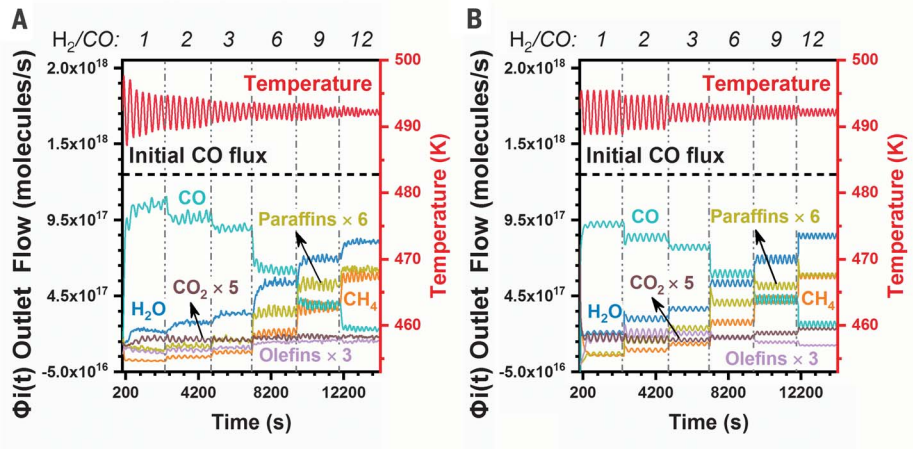

Fig. 5. Experimental and theoretical flow rates under conditions of self-sustained nonisothermal oscillations and forced temperature oscillations. (**A**) Time evolution of temperature and outlet flows under the same experimental conditions as in Fig. 2. (**B**) The same variables simulated with the theoretical kinetic model described in the supplementary materials for forced temperature oscillations. The outlet flow of CO is out of phase with temperature and products for the theoretical model in (B) as well as for the experimental observations in (A).

Co/Mn–oxide (*16*), and other catalyst compositions. The respective kinetic evidence for Co/Ce–oxide is also provided in the supplementary materials.

Chain lengthening involves surface hydrogenation of formate followed by CO insertion into the nascent surface O–R bond, where R is an alkyl group. Repetitive partial hydrogenation of surface carboxylate and CO insertion into the respective alkoxy O–R bond then provides chain lengthening. The reaction scheme also considers CO_2 formation from surface formate and may be completed to allow for olefin formation and hydrocarbon functionalization.

An essential feature of our reaction mechanism is the relatively late water rejection from the adsorbed layer. This result is in full agreement with results obtained from chemical transient kinetics for various catalyst systems (*14*, *16*, *44*). In the case of Co/Ce–oxide, fig. S2 shows delay times for water formation of several hundred seconds as compared with several seconds for methane formation. Reversible Ce^{4+}-to-Ce^{3+} reduction has not been considered in our reaction scheme nor has a Co-to-Co_2C transformation been accounted for. Including such structural changes in a complex kinetic reaction scheme like the FT reaction is challenging. Furthermore, no experimental evidence to support the occurrence of these transformations under atmospheric reaction conditions, as applied in our study, has been obtained (for details, see the supplementary materials).

Figure 5 compares the results of forced temperature oscillations with self-sustained nonisothermal oscillations as observed experimentally. The temperature dependence was assumed to arise mainly from Arrhenius factors associated with C–O bond breaking. The level of agreement between the two is deemed to be excellent. Time-averaged outlet flows of reactants and products deviate by about 20% (and usually much less) from each other over the entire range of H_2/CO ratios. We note that this level of agreement is strongly dependent on the values of the kinetic constants that are used (see supplementary materials). Earlier observations of large-amplitude (100° to 200°C) and very-long-period (usually 60 to 80 min) oscillations in the FT reaction at higher pressures (10 to 22 bar) did not provide deep mechanistic understanding (*34*, *45*). In addition to heat- and mass-transfer limitations, reversible deactivation through carbon deposition (*34*, *46*) and oxidation-reduction cycles were suggested to provide a chemical feedback for oscillations in temperature and either in-phase CO (*45*) or out-of-phase CO conversion (*34*).

Discussion

We report the discovery of rate-and-selectivity oscillations in the FT reaction over cobalt/ceria catalysts. The observations are modeled with a kinetic scheme based on the CO insertion mechanism, the thermal activation of C–O bond breaking, and periodic temperature forcing. Previous kinetic modeling studies that used the concept of forced oscillations to replicate self-sustained oscillatory behavior have generally been on much-less-complicated reaction networks. Ultimately, it would be of interest to generate self-sustained oscillatory behavior on the basis of a thermokinetic feedback mechanism without forcing the temperature to oscillate.

From an experimental point of view, the use of a nearly gradient-free microreactor turned out to be advantageous for our mean-field kinetic modeling. Although heat transport through the gas phase ensures "global" synchronization over the catalyst bed, local coverages at the surface of individual particles may vary greatly, thus causing surface diffusion and spatiotemporal self-organization. Such phenomena have been studied in great detail under isothermal and ultrahigh vacuum conditions with oriented single crystals (*47*) but escape detectability in ensemble-averaging analyses with support catalysts at ambient pressures. With regard to the FT reaction, kinetic studies under molecular flow conditions in ultrahigh vacuum are incongruous because of the strong pressure dependence related to the hydrogen reactant.

We anticipate that our approach will spawn further research to determine the appropriate parameters for triggering and analyzing kinetic instabilities of catalytic reactions that are as complicated as the FT reaction. This discovery can provide insight into the reaction pathways that lead to paraffins and olefins over a wide range of H_2/CO partial pressure ratios and benefit present FT research, up to the point of astrochemistry, where the reaction is being considered as a candidate for producing complex molecules from simpler ones (*48*–*50*). The results of our studies reinforce the concept of a dynamic catalyst design (*51*) to improve the performance in terms of rate and selectivity by using oscillatory reaction states. Concurrent theoretical analyses under thermokinetic conditions may guide the mechanistic understanding of reactions that are as complex as the FT synthesis.

REFERENCES AND NOTES

1. BASF, "Verfahren zur Darstellung von Kohlenwasserstoffen und deren Derivaten," German Patent 293,787 (1913).
2. F. Fischer, H. Tropsch, *Brennst. Chem* **4**, 276–285 (1923).
3. H. A. Bahr, V. Jessen, *Berichte der Dtsch. Chem. Gesellschaft A B Ser.* **63**, 2226–2237 (1930).
4. S. Weller, L. J. E. Hofer, R. B. Anderson, *J. Am. Chem. Soc.* **70**, 799–801 (1948).
5. R. B. Anderson, W. K. Hall, A. Krieg, B. Seligman, *J. Am. Chem. Soc.* **71**, 183–188 (1949).
6. J. A. Amelse, J. B. Butt, L. H. Schwartz, *J. Phys. Chem.* **82**, 558–563 (1978).
7. J. W. Niemantsverdriet, A. M. Van Der Kraan, W. L. Van Dijk, H. S. Van Der Baan, *J. Phys. Chem.* **84**, 3363–3370 (1980).
8. M. Claeys *et al.*, *J. Catal.* **318**, 193–202 (2014).
9. Y. Xiang, N. Kruse, *Nat. Commun.* **7**, 13058 (2016).
10. L. Zhong *et al.*, *Nature* **538**, 84–87 (2016).
11. Y. An *et al.*, *J. Catal.* **366**, 289–299 (2018).
12. Z. Zhao *et al.*, *ACS Catal.* **8**, 228–241 (2018).
13. J. A. Christiansen, "Method of producing methyl alcohol from alkyl formates," US Patent 1,302,011 (1919).
14. J. Schweicher, A. Bundhoo, N. Kruse, *J. Am. Chem. Soc.* **134**, 16135–16138 (2012).
15. M. Zhuo, K. F. Tan, A. Borgna, M. Saeys, *J. Phys. Chem. C* **113**, 8357–8365 (2009).
16. M. Athariboroujeny *et al.*, *ACS Catal.* **9**, 5603–5612 (2019).
17. R. A. van Santen, A. J. Markvoort, *ChemCatChem* **5**, 3384–3397 (2013).
18. B. Todic, W. Ma, G. Jacobs, B. H. Davis, D. B. Bukur, *Catal. Today* **228**, 32–39 (2014).
19. J. Hindermann, G. Hutchings, A. Kiennemann, *Catal. Rev. Sci. Eng.* **35**, 1–127 (1993).

20. S. Storsæter, D. Chen, A. Holmen, *Surf. Sci.* **600**, 2051–2063 (2006).
21. Y. Xiang *et al*., *J. Am. Chem. Soc.* **135**, 7114–7117 (2013).
22. G. R. Johnson, S. Werner, A. T. Bell, *ACS Catal.* **5**, 5888–5903 (2015).
23. Z. Li *et al*., *ACS Catal.* **7**, 3622–3631 (2017).
24. J. Paterson *et al*., *ChemCatChem* **10**, 5154–5163 (2018).
25. Y. Xiang, L. Kovarik, N. Kruse, *Nat. Commun.* **10**, 3953 (2019).
26. M. K. Gnanamani *et al*., *Appl. Catal. A Gen.* **393**, 17–23 (2011).
27. P. Wang *et al*., *Ind. Eng. Chem. Res.* **61**, 3900–3909 (2022).
28. L. Spadaro *et al*., *J. Catal.* **234**, 451–462 (2005).
29. Y. Liu *et al*., *Fuel* **324**, 124518 (2022).
30. W. T. Figueiredo *et al*., *ACS Appl. Nano Mater.* **2**, 2559–2573 (2019).
31. E. Iglesia, S. L. Soled, R. A. Fiato, *J. Catal.* **137**, 212–224 (1992).
32. P. Hugo, *Berichte der Bunsengesellschaft für Phys. Chemie* **74**, 121–127 (1970).
33. H. Beusch, P. Fieguth, E. Wicke, *Chemieingenieurtechnik* **44**, 445–451 (1972).
34. T. T. Tsotsis, V. U. S. Rao, L. M. Polinski, *AIChE J.* **28**, 847–851 (1982).
35. I. Y. Sal'nikov, *Dokl. Akad. Nauk SSSR* **60**, 405–408 (1948).
36. I. Y. Sal'nikov, *Zh. Fiz. Khim* **23**, 258–272 (1949).
37. I. V. Derevich, *Int. J. Heat Mass Transf.* **53**, 135–153 (2010).
38. M. Ojeda *et al*., *J. Catal.* **272**, 287–297 (2010).
39. K. C. Waugh, *Catal. Today* **15**, 51–75 (1992).
40. F. C. Meunier, *Angew. Chem. Int. Ed.* **50**, 4053–4054 (2011).
41. Y. Yang, C. A. Mims, R. S. Disselkamp, C. H. F. Peden, C. T. Campbell, *Top. Catal.* **52**, 1440–1447 (2009).
42. D. Lorito, A. Paredes-Nunez, C. Mirodatos, Y. Schuurman, F. C. Meunier, *Catal. Today* **259**, 192–196 (2016).
43. J. Schweicher *et al*., *J. Phys. Chem. C* **114**, 2248–2255 (2010).
44. A. Bundhoo, J. Schweicher, A. Frennet, N. Kruse, *J. Phys. Chem. C* **113**, 10731–10739 (2009).
45. L. Caldwell, in *Inst. Chem. Eng. Symp. Ser. 87* (1984), pp. 151–158.
46. M. M. Slin'ko, N. I. Jaeger, in *Oscillating Heterogeneous Catalytic Systems*, vol. 86 of *Studies in Surface Science and Catalysis* (Elsevier, 1994), chap. 4.
47. R. Imbihl, G. Ertl, *Chem. Rev.* **95**, 697–733 (1995).
48. M. H. Studier, R. Hayatsu, E. Anders, *Geochim. Cosmochim. Acta* **32**, 151–173 (1968).
49. E. Anders, R. Hayatsu, M. H. Studier, *Science* **182**, 781–790 (1973).
50. M. E. Kress, A. G. G. M. Tielens, *Meteorit. Planet. Sci.* **36**, 75–91 (2001).
51. M. Shetty *et al*., *ACS Catal.* **10**, 12666–12695 (2020).

ACKNOWLEDGMENTS

Funding: R.Z. acknowledges financial support from Chambroad Chemical Industry Research Institute Co., Ltd. R.Z. and Y.W. acknowledge financial support from the US Department of Energy Basic Energy Sciences Catalysis Science program, grant DE-FG02-05ER15712. N.K. thanks the National Science Foundation for financial support under contract no. CBET-1438227. **Author contributions:** R.Z. performed the experiments and contributed to the drafting of the manuscript. Y.W. provided advice and contributed to the final drafting of the manuscript. P.G. performed the theoretical calculations and contributed to the drafting of the manuscript. N.K. initiated and supervised the project and also took the lead in drafting the manuscript. **Competing interests:** The authors declare no competing interests. **Data and materials availability:** All data needed to evaluate the conclusions in the paper are present in the paper or the supplementary materials.

SUPPLEMENTARY MATERIALS

science.org/doi/10.1126/science.adh8463
Materials and Methods
Supplementary Text
Figs. S1 to S7
Table S1
References (*52*–*55*)

Submitted 20 March 2023; accepted 18 August 2023
10.1126/science.adh8463